arXiv:1906.10231v1 [physics.bio-ph] 19 Jun 2019

Environment-Assisted Quantum Photo-Protection in Interacting Multi-Exciton Transfer Complexes

Elinor Zerah-Harush and Yonatan Dubi*

Department of Chemistry and the Ilse Katz Center for nanoscale Science and Technology, Ben-Gurion University of the Negev, Beer Sheva, Israel

E-mail: jdubi@bgu.ac.il

Abstract

Transport of excitons through transfer networks is a unique example where the interplay between quantum coherence and environment-induced dephasing leads to non-trivial effects. One exciting example is the environment-assisted quantum transport, (ENAQT), where, counter intuitively, the environment interrupts quantum transport in a way that enhances the transfer efficiency. Here we show that the interplay between dephasing and quantum coherence can lead to an additional function in exciton transport - photo-protection, that is the reduction of current upon increased excitation. We start by demonstrating that even under weak coupling conditions, weak excitations can lead to multiple-exciton generation, thus going beyond the common single-exciton approximation. We then consider the transport of two excitons, and show that a interplay between dephasing and exciton-exciton interactions leads to a reduction in current, i.e. to photo-protection. The effect may be related to actual photo-protection observed in photosynthetic systems.

Exciton networks are structures that allow for energy transfer, utilized by nature in the photosynthetic process, where solar-energy is captured and directed toward its target.[1,2] This energy is carried by an exciton (an electron-hole pair), created as a consequence of electron excitation in the capturing complex - the antenna. The exciton travels through the network until it reaches the reaction center, where the chemical reactions are executed. The total transport from exciton formation to exciton absorption by the reaction center was found to have an extremely high yield ($\sim 95\%$).[3] This high yield casts doubt on the accepted Forester mechanism,[3,4] wherein the excitons are treated as particles that "hop" from one molecule to another.[5]

A possible explanation for the high yield was put forward following nonlinear spectroscopy experiments that were conducted several years ago, which showed indications for long-lived oscillatory signals.[6–9] These were conjectured to be of a quantum mechanical origin, marking the presence of quantum coherence in these systems, which contribute to the high yield. The presence of quantum coherence in biological system is highly unexpected since it is usually easily disturbed by the biological environment (they are, simply put, presumed to be too hot and wet for quantum coherence). It is thus not surprising that the prospect of quantum coherence in biological systems raised much excitement (and debate).[4,10–18]

The idea that exciton motion is affected by an interplay of both quantum and classical dynamics requiers a theory that can account for both. Such theories were put forward in recent years, adopting an open-quantum systems approach (in particular Lindblad[19–22] or Redfield theory[23]). A common feature that comes up in many works is that of *environment-assisted quantum transport* (ENAQT), namely the concept that under certain conditions, the efficiency of quantum transport can in fact increase under the influence of an environment (which drives the exciton towards classical dynamics). Its central hallmark is a maximum in the exciton current not when the system is environment-free, but rather when the environment induces a finite (but not too large) dephasing on the system.[19–21,24–26] This efficiency enhancement is rather universal, and is an outcome of the interplay between quantum and

classical dynamics, as was recently demonstrated in Ref. 24, and may be the explanation for high yield attributed to exciton networks.

The study of ENAQT and the exciton-environment interplay is challenging to model. Thus, a few accepted assumptions are often made. First, the system is assumed to have no memory (Markov approximation[27,28]). Second, system-environment coupling is considered weak (Born approximation[27]). In many cases, the assumption of weak interaction between source and system is translated into a third assumption - that the system is only occupied by one exciton. Here, we challenge this assumption, and show that even under mild conditions (and commonly-used parameters) the single-exciton limitation is flawed, as the system has a high probability of being occupied by two excitons. Such two-exciton states may play an important role in exciton transport,[29] especially in the presence of exciton interactions, which were observed by coherent two-dimensional spectroscopic,[30] emphasizing the importance of considering them in theoretical models.

Our results and analysis are based on calculation of exciton currents through a quantum network subjected to an exciton source and drain and a dephasing environment, the methodology being similar to that of Ref. 20 and 24. The exciton network Hamiltonian is described by a tight-binding chain of length L, $\mathcal{H} = \sum_{i=1}^{L} \epsilon_i e_i^\dagger e_i - t \sum_{i,j=1, i\neq j}^{L} e_i^\dagger e_j$, where $e_i^\dagger(e_i)$ creates (annihilates) an exciton at site i, t is the hopping matrix elements (limited to nearest neighbors). The dynamics are described within the Lindblad quantum master equation, $\dot{\rho} = -\frac{i}{\hbar}[\mathcal{H}, \rho] + \sum_k \left(V_k \rho V_k^\dagger - \frac{1}{2}\{V_k^\dagger V_k, \rho\} \right)$,[21,31] where ρ is the density matrix and V_k are a list of Lindblad operators encoding the action of the environment on the exciton system. The Lindblad operators for dephasing operate on each site via $V_i = (\gamma_{deph})^{1/2} e_i^\dagger e_i$. Exciton injection and extraction are defined by Lindblad operators $V_{inj} = (\gamma_{inj})^{1/2} e_{i_{inj}}^\dagger$ and $V_{ext} = (\gamma_{ext})^{1/2} e_{i_{ext}}$. The rates γ_{deph}, γ_{inj} and γ_{ext} are the exciton dephasing, injection and extraction rates, respectively, and i_{inj} and i_{ext} are the indices of the sites where injection and extraction take place, respectively. The exciton current and populations are evaluated at the steady state, which is relevant for natural systems illuminated by incoherent light.[32–34] The

steady-state density matrix ρ_S, from which all the relevant quantities (currents, populations) are calculated,[20,24] is evaluated as the kernel of the Lindbladian super-operator.

As pointed above, the approximation of singly-occupied systems is common in the study of exciton networks. In order to examine the validity of this approximation, we start by calculating the average number of excitons $\langle N \rangle$ in an exciton chain connected to the source and drain at the edges. The average occupation can be found analytically if the chain is limited to the ocupation of a single exciton (see supplementary information for further details), $\langle N \rangle = \frac{\gamma_{inj}}{\gamma_{ext}} \left(\frac{\gamma_{inj}}{\gamma_{ext}} + K^{-1} \right)^{-1}$ where $K = c_1 + c_2(\frac{\gamma_{ext}}{t})^2 + c_3(\frac{\gamma_{deph}\gamma_{ext}}{t^2})$, with c_1, c_2, c_3 constants that depends solely on L (number of sites).

This result shows that the most important parameter controlling the average exciton number, is the injection-extraction rates ratio (IERR), $\frac{\gamma_{inj}}{\gamma_{ext}}$, (especially if t is larger than the extraction and dephasing rates, which is indeed the case for biological systems[21,35,36]). If the IERR is large, one expects that there will be many excitons occupying the newtork at the same time. A simple classical analogy is a bucket which is continuously filled with water (through, say, a hose) and emptied from water (say, via a hole at its bottom). The water level in the bucket will be determined by the ratio of rates at which water is poured in and out of it.

What happens if one goes beyond the single-exciton approximation? To explore this, in figure 1 we show the average number of excitons occupying the system (the middle solid line) as a function of IERR in a wire of five sites, occupied by up to two excitons (the hopping element is taken as $t = 60\text{cm}^{-1}$, which is relevant to natural systems[21,35,36]). As expected, the average number of excitons increases with the IERR, and exceeds the value of $\langle N \rangle = 1$ for IERR$= 0.22$. In addition, the standard deviation is shown as error bars above and below the $\langle N \rangle$ curve, pointing on the presence of more then one exciton even for surprisingly small IERR, much smaller than the typical value of IERR~ 1 used in previous works.

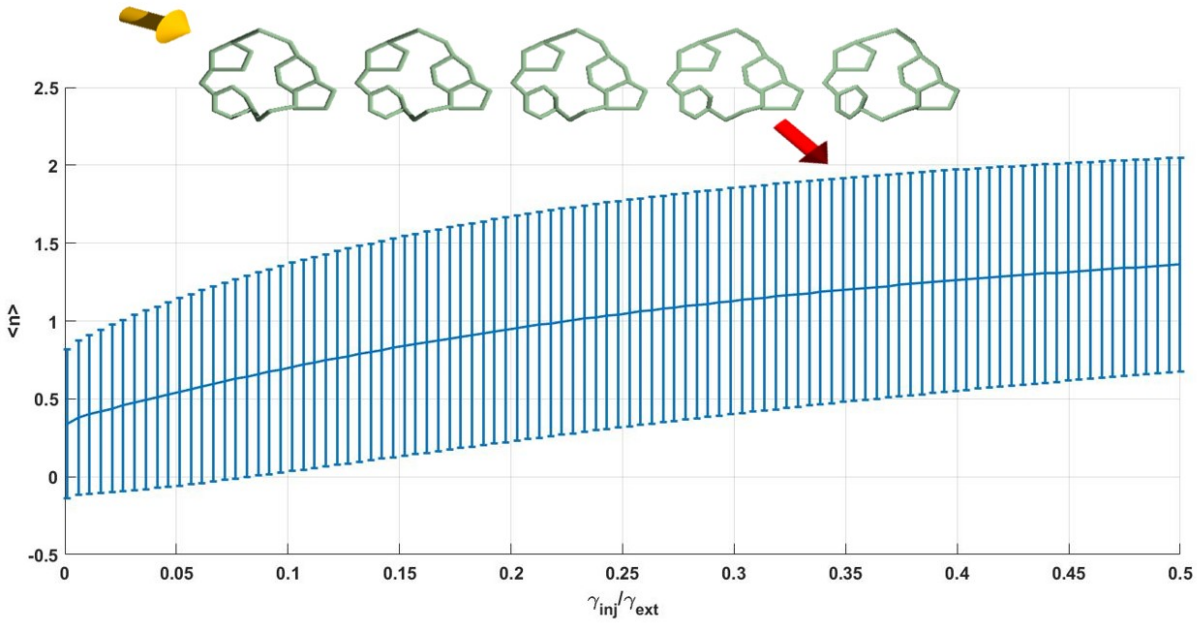


Figure 1: Average exciton number $\langle N \rangle$ as a function of the IERR, $\frac{\gamma_{inj}}{\gamma_{ext}}$, for a system of five sites as depicted in the inset cartoon. Error bars depict the total density fluctuations. These results imply that two-exciton states are present and may even be dominant, even for parameters where only single-exciton occupation was perceived.

What would be the effect of double exciton occupancy? one can borrow intuition from electron transport, where it is well-known that electron interactions can dramatically affect transport. Similarly, one could expect exciton-interactions to dramatically affect the transport properties of exciton networks. To take exciton interactions into account, we add to the Hamiltonian an interaction term of the form $H_{int} = \sum_i U \hat{n}_i \hat{n}_{i+1} + h.c.$, where $\hat{n}_i = e_i^\dagger e_i$ and U is the interaction strength (the interaction is limited to nearest-neighbors for simplicity).

As mentioned above, a central feature of ENAQT is a maximum in the current-dephasing curve. It is thus important to understand how this dependence is affected by exciton interactions. In Fig. 2 we show the exciton current as a function of dephasing rate, for different values of interaction strength $U = 0, 1000, 2500, 5000$ ps^{-1}. We study a system of five sites,

with injection from the first site and extraction from the fourth site. Parameter values were chosen to be $\gamma_{inj} = 0.01$ ps^{-1},$\gamma_{ext} = 1$ ps^{-1}, $\epsilon_i = 135000$ cm^{-1}, and $t = -60$ cm^{-1}(these values are maintained unless mentioned otherwise). These parameters were carefully chosen to be within the two-exciton limit (but we made sure that the probability of exciting three excitons is extremely small).

In the absence of exciton interactions (blue curve in Fig. 2), ENAQT is observed even when two excitons are occupying the system. However, as the interaction strength increases (orange, green and red lines), the behavior changes qualitatively, reversing the trend from an environment-*assisted* transport, to an environment-*hampered* transport.

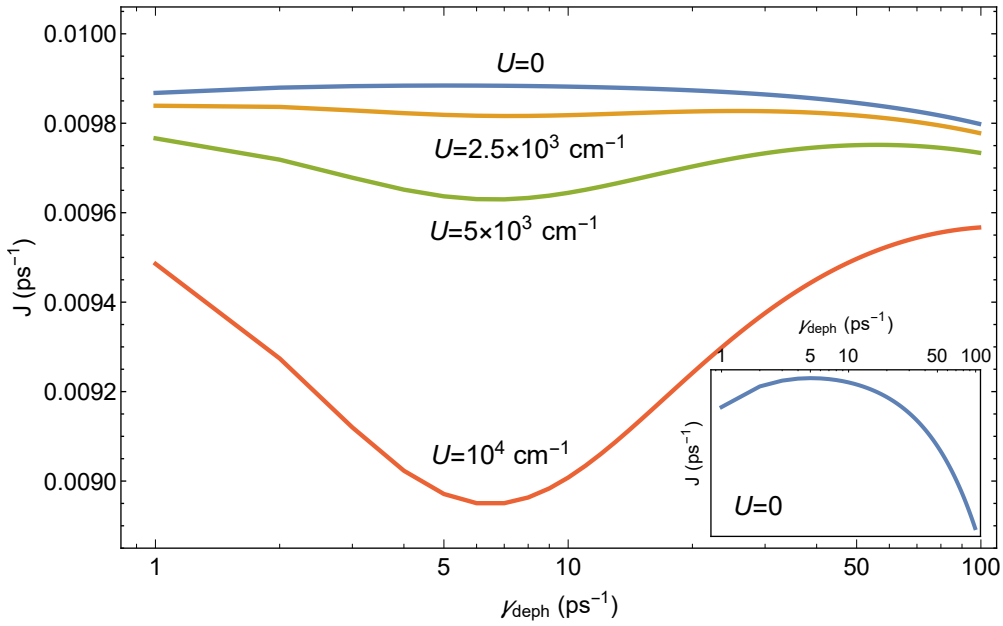


Figure 2: Exciton current as a function of γ_{deph} for different values of exciton interaction strength (see text for numerical parameters). A qualitative change of behaviour is observed, from ENAQT to environment-hamperd transport. Inset: Exciton current as a function of γ_{deph} enlarged, emphasizing the appearance of ENAQT for $U = 0$.

To elucidate the origin of this effect, we note that it is strongest at the same dephasing rates at which the current-enhancement is strongest in the absence of interactions, thus indicating that they have a similar origin. As shown in Ref. 24, ENAQT appears due to the competition between two dephasing-induced processes, (1) a "density flattening" effect, where the density of exitons (along the chain) tends to be smoothed out by dephasing towards

the average density, and (2) the generation of a density gradient (leading to Fick's law at the strong dephasing - i.e. classical - limit). It is thus natural to examine what happens to the local exciton density as exciton interactions are increased. In Fig. 3(a-c) we plot the local exciton density (blue, yellow, green, red and purple correspond to sites 1 to 5, respectively), as a function of dephasing rate. In dashed gray line we show the corresponding exciton current (same data of Fig. 2). In the absence of interactions ($U = 0$, Fig. 3(a)) the densities show the flattening effect, and coalesce towards the average density, thus minimizing the density inter-site fluctuations $\Delta_n = \frac{1}{L}\sum_i (n_i - \bar{n})^2$ at the dephasing rate of maximal current. Further increase in dephasing rate leads to the formation of a (classical) density gradient. This is a manifestation of the competition between the tendency of dephasing to generate a density gradient vs its tendency to reduce density fluctuations.

As interactions increase ($U = 5000, 1000\text{cm}^{-1}$, Figs. 3(b-c)), one sees a qualitative change in this behavior. At what was the optimal dephasing rate, the density now tends to be scattered (i.e. generate the largest variations in density between different sites on the chain). This could be imagined as simply related to the Coulomb repulsion, which favors density fluctuations as to minimize the total energy. This is indeed the origin of the effect, but is not the whole story, because an important part is played by the connection to the source and drain, which forces the system to always generate density fluctuations such that the density at the extraction site is reduced (see supplementary for more details).

As a result of the increase in the scatter of occupations, the density at the exit site (connected to the exciton drain) is pushed to lower and lower values with increasing interaction strength, leading to a reduction in current.[24] This is depicted in Fig. 3(d), where we plot the inter-site density fluctuations Δ_n (not to be confused with the statistical standard variation of the density, Δ_n is a measure of the fluctuations in density over real space) as a function of dephasing rate. A clear change in trend is evident, from a local minimum in Δ_n at $U = 0$ (blue line) towards a local maximum in Δ_n for increasing values of U (yellow, green and red lines).

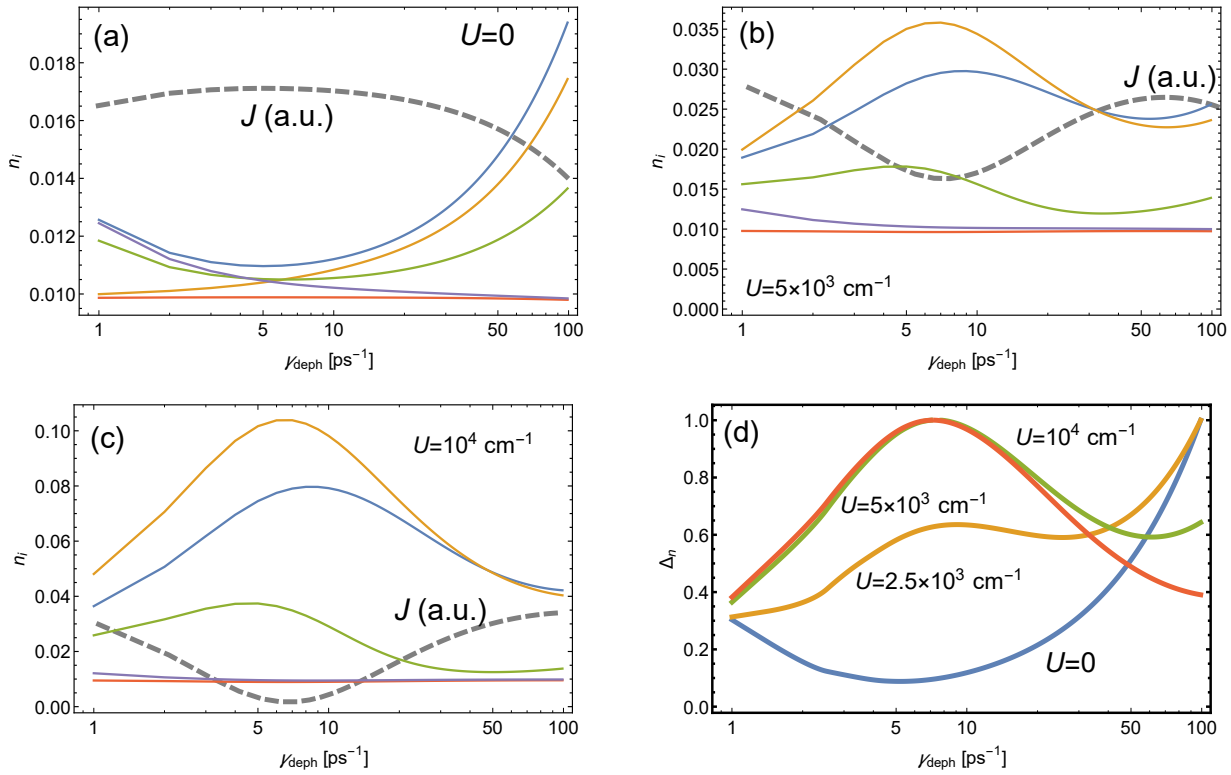


Figure 3: (a-c) local exciton density of sites 1-5 (blue, yellow, green, red and purple lines) as a function of dephasing rate, for increasing values of interaction strength $U = 0, 5000, 10000$ cm^{-1}. A qualitative change in behavior is observed, and the density goes from flattening to broadening at optimal dephasing rate. Dashed gray lines show the exciton current (in arbitrary units). (d) inter-site density variation Δ_n as a function of dephasing rate for different interaction strengths.

So far, we discussed two effects: (i) the appearance of two-excitons states under (relatively) strong injection and (ii) the decrease in current in the presence of exciton-exciton interactions and dephasing. Next, we show that combining the two effects leads to what we describe as environment-assisted quantum photo-protection (QPP). Photo-protection (especially in the form of non-photochemical quenching) is the situation in which an increase in the excitation (for instance when the solar illumination is strong) results in a decrease in current, and is a mechanism with which the photosynthetic apparatus is kept from being overheated and burnt.[37–42] Possible relation between quantum coherence, environmental effects and non-photochemical quenching was studied recently within the single-exciton limit.[43–45]

Within the model presented here, increased solar illumination corresponds to an increase

in exciton injection, i.e. in γ_{inj}. The mechanism for QPP is thus the following; for weak exciton injection, the exciton network is singly-occupied. In this regime, ENAQT is at play and the current is enhanced by the environment. As the exciton injection rate increases, the probability of having two excitons excited in the network increases, finally being the dominant configuration. At this regime, the interplay of dephasing and interaction leads to the reduction in the current described above.

To demonstrate this, in Fig. 4 we plot the exciton current as a function of the IERR (which is proportional to the injection rate), for three different regimes, the quantum regime (no dephasing), ENQAT regime (intermediate dephasing, $\Gamma_{deph} = 5\text{ps}^{-1}$), and classical regime (strong dephasing, $\Gamma_{deph} = 100\text{ps}^{-1}$) . In Fig. 4(a) we consider the case where no exciton-exciton interactions are present ($U = 0$). In this case, the system behaves similarly to the one-exciton system, and hence no QPP. In Fig. 4(b) the case of strong interactions ($U = 5000\text{cm}^{-1}$) is shown. Here, the current is reduced in the ENAQT regime, leading to the environment-assisted QPP.

Finally, we note that the QPP effect shown above is rather general, and in similarity to ENAQT,[24] is not limited to 1D chains but can appear basically for any geometry. Of particular relevance to the topic at hand, in the supplementary information we show the QPP for the Fenna-Metthews-Olson complex, which has a non-trivial geometry.[20,35] Similar results were obtained for ringed structures and various other geometries.

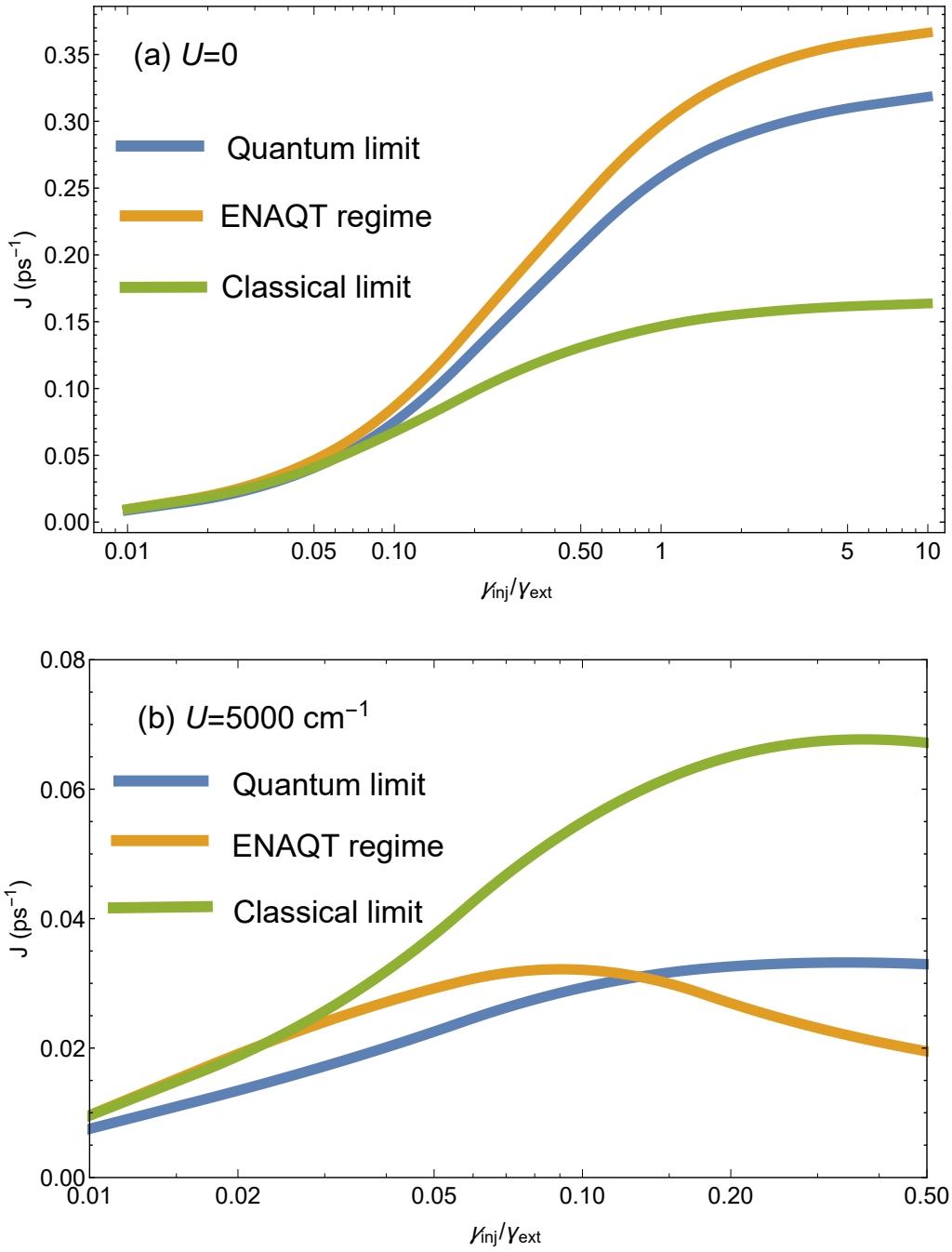


Figure 4: (a) Current as a function of IERR, $\gamma_{inj}/\gamma_{ext}$, with no exciton-exciton interactions ($U = 0$) at different dephasing regimes: classic limit (Green curve, $\gamma_{deph} = 200$ cm^{-1}), ENAQT (Orange curve, $\gamma_{deph} = 5$ cm^{-1}) and quantum limit (Blue curve,$\gamma_{deph} = 0.001$ cm^{-1}). (b) Same as (a) for $U = 5000$ cm^{-1}.

In summary, we demonstrated that a combination of dephasing and exciton interac-

tions leads, under certain conditions, to the appearance of quantum photo-protection. The possibility of interplay between quantum dynamics and environmental effects in the photosynthesis process has already generated much interest, but was only limited to a single function, namely increasing the exciton transfer efficiency. Our results thus add another function that arises from such interplay. The model presented here can be generalized to include more detailed aspects of the environment (which can be encoded into the vibrational spectral function and used within a Redfield approach[23]) and a self-consistent evaluation of the relation between exciton transfer currents and heating. Such studies will further illustrate the relation between quantum coherence, classical dynamics and performance in photosynthetic systems.

References

(1) Mohseni, M.; Omar, Y.; Engel, G. S.; Plenio, M. B. *Quantum Effects in Biology*; Cambridge University Press, Google-Books-ID: oIf2AwAAQBAJ.

(2) Molecular Mechanisms of Photosynthesis, 2nd Edition. `https://www.wiley.com/en-us/Molecular+Mechanisms+of+Photosynthesis%2C+2nd+Edition-p-9781405189767`.

(3) Levi, F.; Mostarda, S.; Rao, F.; Mintert, F. Quantum mechanics of excitation transport in photosynthetic complexes: a key issues review. *78*, 082001.

(4) Fleming, G. R.; Scholes, G. D. Quantum mechanics for plants. *431*, 256.

(5) Govorov, A.; Martnez, P. L. H.; Demir, H. V. *Understanding and Modeling Frster-type Resonance Energy Transfer (FRET): Introduction to FRET, Vol. 1*; Nanoscience and Nanotechnology; Springer Singapore.

(6) Engel, G. S.; Calhoun, T. R.; Read, E. L.; Ahn, T.-K.; Manal, T.; Yuan-Chung Cheng,;

Blankenship, R. E.; Fleming, G. R. Evidence for wavelike energy transfer through quantum coherence in photosynthetic systems. *446*, 782–786.

(7) Collini, E.; Wong, C. Y.; Wilk, K. E.; Curmi, P. M. G.; Brumer, P.; Scholes, G. D. Coherently wired light-harvesting in photosynthetic marine algae at ambient temperature. *463*, 644–U69, WOS:000274193900032.

(8) Panitchayangkoon, G.; Hayes, D.; Fransted, K. A.; Caram, J. R.; Harel, E.; Wen, J.; Blankenship, R. E.; Engel, G. S. Long-lived quantum coherence in photosynthetic complexes at physiological temperature. *107*, 12766–12770.

(9) Romero, E.; Augulis, R.; Novoderezhkin, V. I.; Ferretti, M.; Thieme, J.; Zigmantas, D.; Van Grondelle, R. Quantum coherence in photosynthesis for efficient solar-energy conversion. *Nature physics* **2014**, *10*, 676.

(10) Collini, E. Spectroscopic signatures of quantum-coherent energy transfer. *42*, 4932–4947, WOS:000319527400007.

(11) Lambert, N.; Chen, Y.-N.; Cheng, Y.-C.; Li, C.-M.; Chen, G.-Y.; Nori, F. Quantum biology. *9*, 10–18.

(12) Ishizaki, A.; Fleming, G. R. In *Annual Review of Condensed Matter Physics, Vol 3*; Langer, J. S., Ed.; Annual Reviews, Vol. 3; pp 333–361, WOS:000301793100015.

(13) Pachon, L. A.; Brumer, P. Computational methodologies and physical insights into electronic energy transfer in photosynthetic light-harvesting complexes. *14*, 10094–10108, WOS:000305965200002.

(14) Keren, N.; Paltiel, Y. Photosynthetic energy transfer at the quantum/classical border. *Trends in plant science* **2018**, *23*, 497–506.

(15) Maiuri, M.; Ostroumov, E. E.; Saer, R. G.; Blankenship, R. E.; Scholes, G. D. Coherent

wavepackets in the Fenna–Matthews–Olson complex are robust to excitonic-structure perturbations caused by mutagenesis. *Nature chemistry* **2018**, *10*, 177.

(16) Thyrhaug, E.; Tempelaar, R.; Alcocer, M. J.; Žídek, K.; Bína, D.; Knoester, J.; Jansen, T. L.; Zigmantas, D. Identification and characterization of diverse coherences in the Fenna-Matthews-Olson complex. *Nature chemistry* **2018**, *10*, 780–786.

(17) Rathbone, H. W.; Davis, J. A.; Michie, K. A.; Goodchild, S. C.; Robertson, N. O.; Curmi, P. M. Coherent phenomena in photosynthetic light harvesting: part twoobservations in biological systems. *Biophysical reviews* **2018**, *10*, 1443–1463.

(18) Reppert, M.; Brumer, P. Quantumness in light harvesting is determined by vibrational dynamics. *The Journal of chemical physics* **2018**, *149*, 234102.

(19) Manzano, D.; Tiersch, M.; Asadian, A.; Briegel, H. J. Quantum transport efficiency and Fourier's law. *86*, 061118.

(20) Dubi, Y. Interplay between Dephasing and Geometry and Directed Heat Flow in Exciton Transfer Complexes. *119*, 25252–25259.

(21) Plenio, M. B.; Huelga, S. F. Dephasing-assisted transport: quantum networks and biomolecules. *10*, 113019.

(22) Chin, A. W.; Datta, A.; Caruso, F.; Huelga, S. F.; Plenio, M. B. Noise-assisted energy transfer in quantum networks and light-harvesting complexes. *12*, 065002.

(23) Jeske, J.; Ing, D. J.; Plenio, M. B.; Huelga, S. F.; Cole, J. H. Bloch-Redfield equations for modeling light-harvesting complexes. *142*, 064104.

(24) Zerah-Harush, E.; Dubi, Y. Universal Origin for Environment-Assisted Quantum Transport in Exciton Transfer Networks. *9*, 1689–1695.

(25) Rebentrost, P.; Mohseni, M.; Kassal, I.; Lloyd, S.; Aspuru-Guzik, A. Environment-assisted quantum transport. *11*, 033003.

(26) Caruso, F.; Chin, A. W.; Datta, A.; Huelga, S. F.; Plenio, M. B. Highly efficient energy excitation transfer in light-harvesting complexes: The fundamental role of noise-assisted transport. *131*, 105106.

(27) Breuer, H.-P. *The Theory of Open Quantum Systems*; Oxford University Press, USA.

(28) Rivas, A.; Plato, A. D. K.; Huelga, S. F.; Plenio, M. B. Markovian master equations: a critical study. *12*, 113032, WOS:000284774900002.

(29) Gurvitz, S.; Berman, G. P.; Sayre, R. T. Multiscale cyclic dynamics in light harvesting complex in presence of vibrations and noise. *The European Physical Journal Special Topics* **2019**, 1–12.

(30) Dostl, J.; Fennel, F.; Koch, F.; Herbst, S.; Wrthner, F.; Brixner, T. Direct observation of excitonexciton interactions. *9*, 2466.

(31) Purkayastha, A.; Dhar, A.; Kulkarni, M. Out of equilibrium open quantum systems: a comparison of approximate Quantum Master Equation approaches with exact results. *93*.

(32) Manzano, D. Quantum transport in networks and photosynthetic complexes at the steady state. *PloS one* **2013**, *8*, e57041.

(33) Tscherbul, T. V.; Brumer, P. Non-equilibrium stationary coherences in photosynthetic energy transfer under weak-field incoherent illumination. *The Journal of chemical physics* **2018**, *148*, 124114.

(34) Pachón, L. A.; Botero, J. D.; Brumer, P. Open system perspective on incoherent excitation of light-harvesting systems. *Journal of Physics B: Atomic, Molecular and Optical Physics* **2017**, *50*, 184003.

(35) Cho, M.; Vaswani, H. M.; Brixner, T.; Stenger, J.; Fleming, G. R. Exciton analysis in 2D electronic spectroscopy. 2005.

(36) Caruso, F. Universally optimal noisy quantum walks on complex networks. *New Journal of Physics* **2014**, *16*, 055015.

(37) Lambrev, P. H.; Miloslavina, Y.; Jahns, P.; Holzwarth, A. R. On the relationship between non-photochemical quenching and photoprotection of photosystem II. *Biochimica et Biophysica Acta (BBA)-Bioenergetics* **2012**, *1817*, 760–769.

(38) Holt, N. E.; Fleming, G. R.; Niyogi, K. K. Toward an understanding of the mechanism of nonphotochemical quenching in green plants. *Biochemistry* **2004**, *43*, 8281–8289.

(39) Derks, A.; Schaven, K.; Bruce, D. Diverse mechanisms for photoprotection in photosynthesis. Dynamic regulation of photosystem II excitation in response to rapid environmental change. *Biochimica et Biophysica Acta (BBA)-Bioenergetics* **2015**, *1847*, 468–485.

(40) Müller, P.; Li, X.-P.; Niyogi, K. K. Non-photochemical quenching. A response to excess light energy. *Plant physiology* **2001**, *125*, 1558–1566.

(41) Demmig-Adams, B.; Garab, G.; Adams III, W.; Govindjee, U. *Non-photochemical quenching and energy dissipation in plants, algae and cyanobacteria*; Springer, 2014; Vol. 40.

(42) Ruban, A. V.; Berera, R.; Ilioaia, C.; Van Stokkum, I. H.; Kennis, J. T.; Pascal, A. A.; Van Amerongen, H.; Robert, B.; Horton, P.; Van Grondelle, R. Identification of a mechanism of photoprotective energy dissipation in higher plants. *Nature* **2007**, *450*, 575.

(43) Berman, G. P.; Nesterov, A. I.; Gurvitz, S.; Sayre, R. T. Possible role of interference, protein noise, and sink effects in nonphotochemical quenching in photosynthetic complexes. *Journal of mathematical biology* **2017**, *74*, 43–76.

(44) Berman, G. P.; Nesterov, A. I.; López, G. V.; Sayre, R. T. Superradiance transition and nonphotochemical quenching in photosynthetic complexes. *The Journal of Physical Chemistry C* **2015**, *119*, 22289–22296.

(45) Berman, G. P.; Nesterov, A. I.; Sayre, R. T.; Still, S. On improving the performance of nonphotochemical quenching in CP29 light-harvesting antenna complex. *Physics Letters A* **2016**, *380*, 1279–1283.